Electronic Supplementary Information

Synergetic Effect of Cu and Graphene as cocatalyst loaded TiO_2 for Enhanced Photocatalytic Hydrogen Evolution from Solar Water Splitting

Xiao-Jun Lv,[*a] Shi-Xiong Zhou,[b] Chen Zhang,[b] Hai-Xin Chang,[c] Yong Chen,[a] and Wen-Fu Fu,[*a,b]

[a] *Key Laboratory of Photochemical Conversion and Optoelectronic Materials and HKU-CAS Joint Laboratory on New Materials, Technical Institute of Physics and Chemistry, Chinese Academy of Sciences, Beijing 100190 (P.R. China), E-mail: xjlv@mail.ipc.ac.cn; fuwf@mail.ipc.ac.cn*

[b] *College of Chemistry and Chemical Engineering, Yunnan Normal University, Kunming, 650092 (P.R. China)*

[c] *WPI-Advanced Institute for Materials Research, Tohoku University, Sendai 980-8578, Japan.*

Contents:

S7: Hydrogen generation capability based on 1.5 % Cu loaded GP 2.0 photocatalysts on H_2 generation evolution in methanol aqueous solution under visible light (λ > 400 nm) by 300 W high press Hg lamp.

S8: Nyquist plots of electrochemical impedance spectra (EIS) for 1.5% Cu loaded on GP electrodes. The EIS measurements were performed in the presence of 1 mM $K_3[Fe(CN)_6]/K_4[Fe(CN)_6]$ (1:1) mixture as a redox probe in 0.1 M KCl aqueous solution.

S9: The on−off photocurrent under Xe lamp illumination) (I without bias in a two−electrode configuration for the (1) 0.5% Cu, (2) 1.0% Cu, (3) 1.5% Cu, (4) 2.0% Cu, (5) 3.0% Cu, (6) 5.0% Cu and (7) 8.0% Cu respectively loaded on GP 2.0 composites as photoanodes in 0.1 M KNO_3 solution.

S10: XPS spectra of Cu 2p in the Cu loaded P25–G composites (1) 8% Cu loaded GP 2.0 before irradiation for hydrogen, (2) 8% Cu loaded GP 2.0 after UV–visible irradiation for 64 h.

References of Supplementary Information

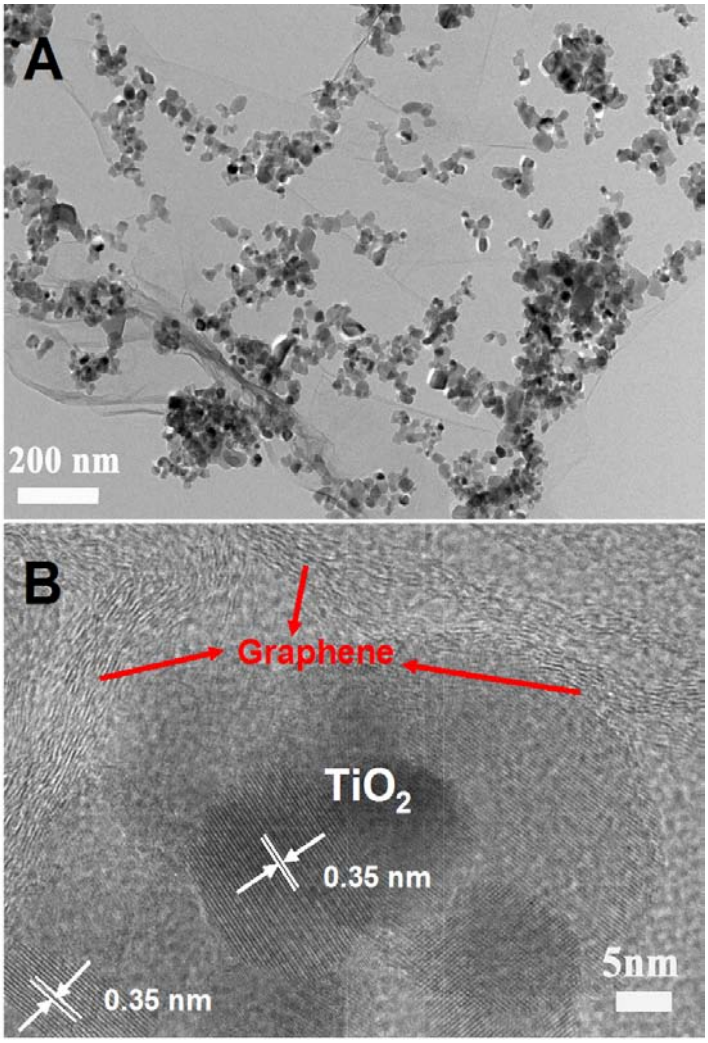

Figure S1. (A) Typical TEM image of GP 2.0 of P25−G composite, with P25 loading on the surface of graphene and concentrating along the wrinkles. (B) High-resolution TEM images of TiO_2 nanoparticles interconnecting with graphene.

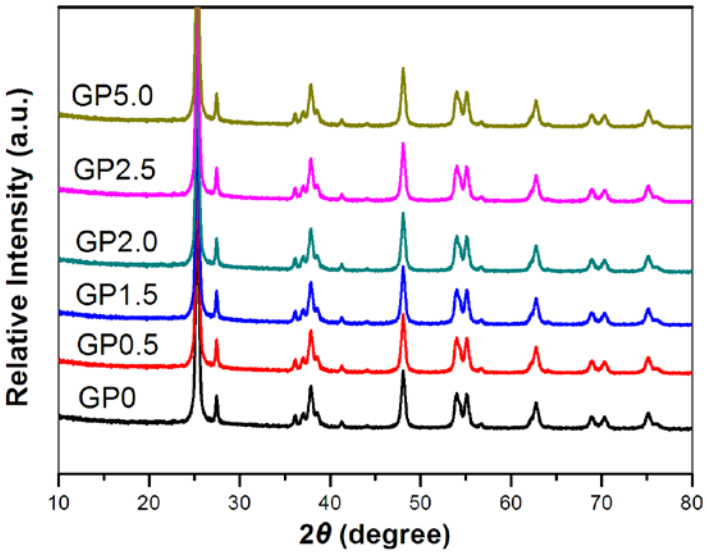

Figure S2. XRD patterns of P25−G composite with different graphene content.

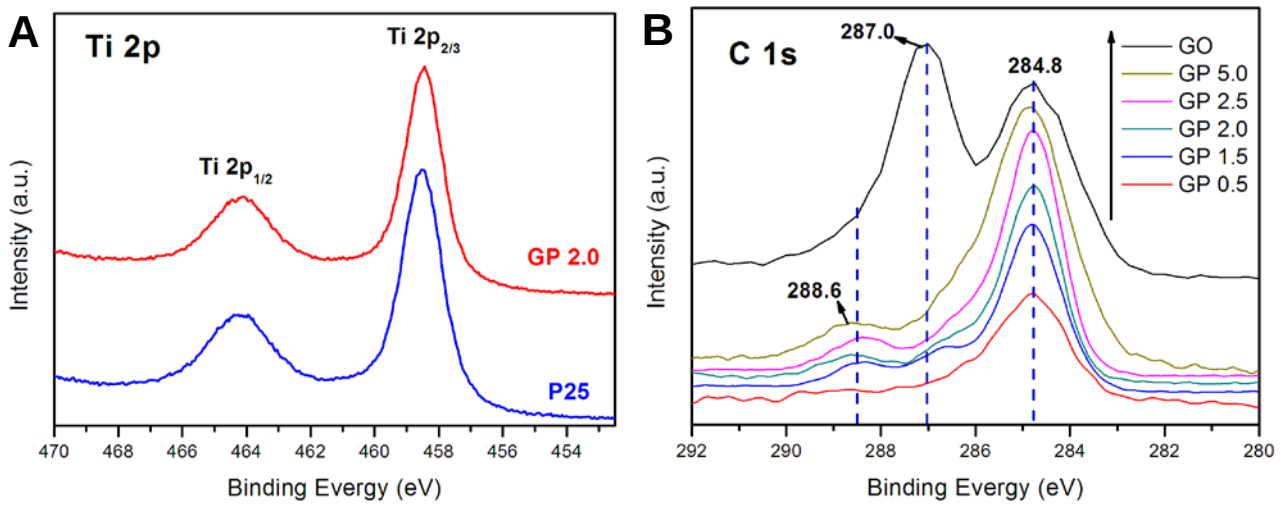

Figure S3. XPS spectra of (A) Ti 2p and (B) C 1s of the graphene oxide (GO) and reduction graphene in P25−G composites with different graphene content.

Figure S3A shows two well resolved peaks at 464.1 and 458.4 eV were observed from the Ti 2p core−level spectrum, which can be assigned to Ti $2p_{1/2}$ and Ti $2p_{3/2}$ spin−orbital components in TiO_2, respectively. And there is no distinct difference between the two spectra of bare P25 and GP 2.0, indicating that the anchoring interaction between graphene and TiO_2 is not the lattice doping.

The C 1s XPS spectra for Graphene oxide (GO) and P25−G with different graphene content composites was shown in Figure S3B. The result show that there was two main peaks were observed in the C 1s spectra of GO, and the peak at 284.8 eV was assignable to the sp^2 carbon species, while the peak at higher binding energies (286−288 eV) was ascribed to oxygenated carbon species such as hydroxyl, carboxyl, and epoxide species on GO surfaces.[1,2] And it is clearly that the peak at 287.0 eV for C–OH group on GO decreases remarkably or disappears in the C 1s XPS spectroscopy of P25−G composites. This indicates that the introduced GO has been efficiently reduced into graphene during the hydrothermal reaction process. In addition, there are relatively weak peak located at 288.6 eV for P25−G composites, which were contributed by carboxyl carbon (O=C–O).[3] Such a surface functional group indicated that the –OH groups on the TiO_2 nanosheets

possibly react with the –COOH groups on the GO surface through esterification to form O=C–O–Ti bonds.[4]

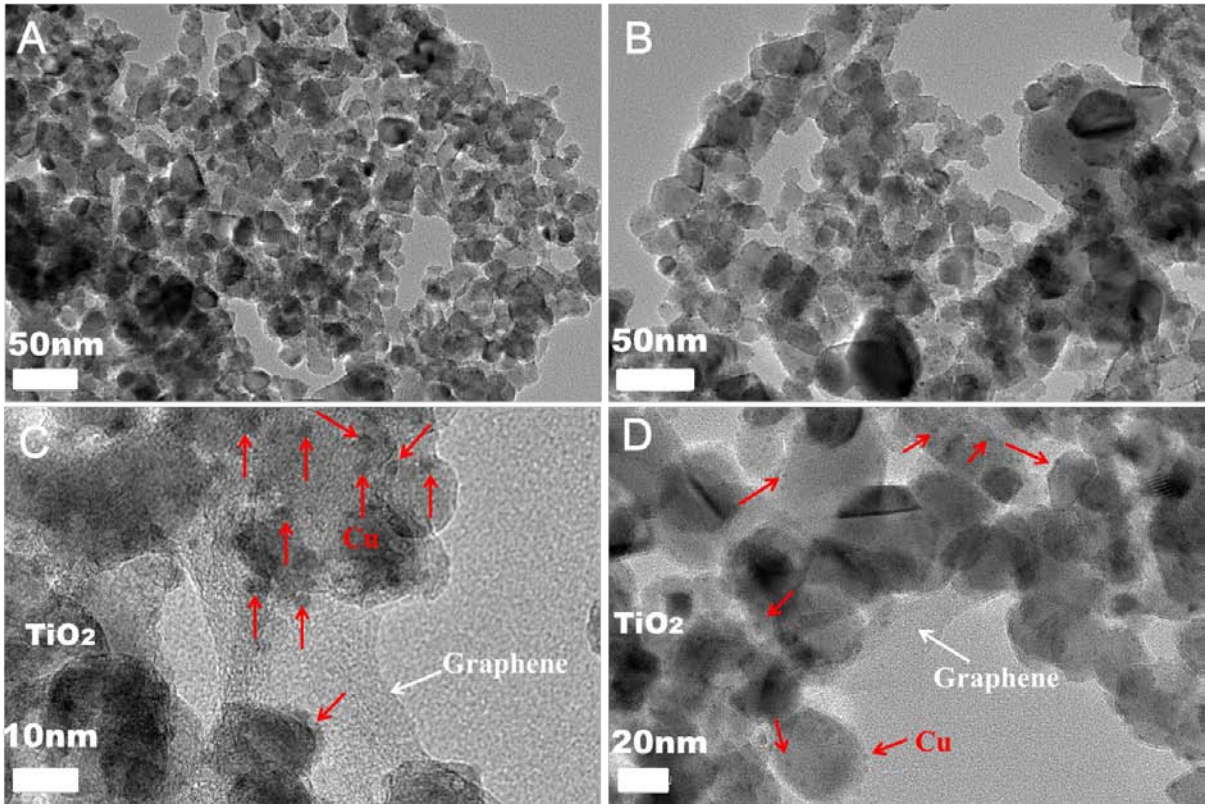

Figure S4. Structural analysis of the photodeposited Cu on GP 2.0 composites. TEM image (A) and HRTEM image (C) of photodeposited 5% Cu on GP 2.0 composites, and different multiple TEM image (B) and (D) of photodeposited 8% Cu on GP 2.0 composites

TEM and HRTEM results clearly show that Cu nanoparticles well dispersed on the surface of TiO_2 and graphene for photodeposited 5% and 8% Cu on GP 2.0 composites in Figure S4. And the well dispersed Cu nanoparticles enhanced the photocatalytic active site for hydrogen generation, simultaneity the close interconnection for TiO_2, Cu, and graphene components would be favor to transfer photogenerated electrons from TiO_2 to Cu and/or graphene sheets, which will increasing the hydrogen evolution.

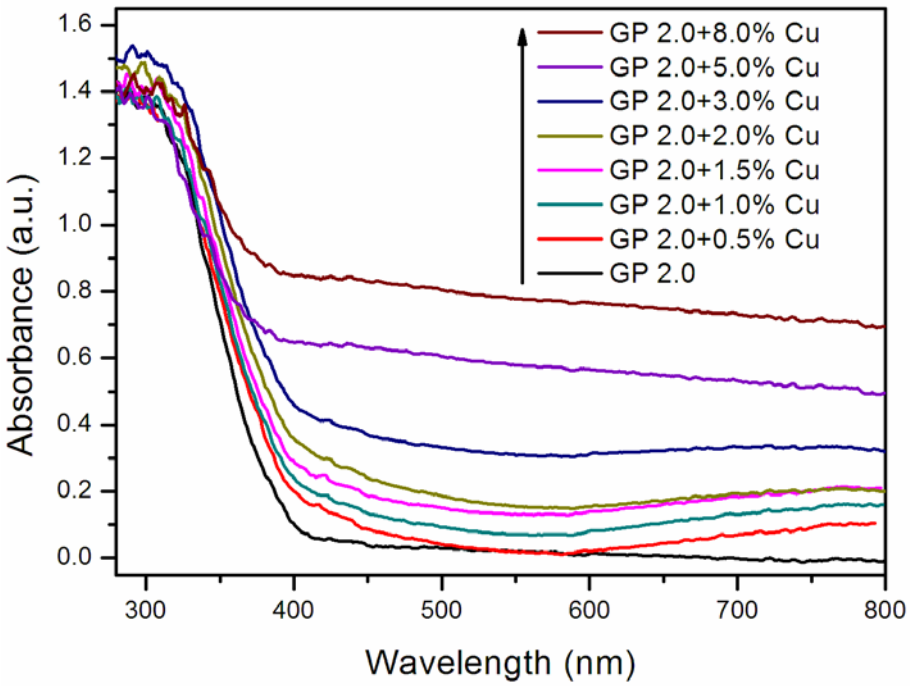

Figure S5. UV–vis diffuse reflection spectrum of GP 2.0 photocatalysts with different copper (wt %) content loading.

UV-vis diffuse reflectione spectrum for the GP 2.0 photocatalysts with different copper (wt %) loading are shown in Figure S5. Compared with the absorption of GP 2.0 photocatalysts, the absorption edge is remarkable red shift after photodeposited different content Cu, and the red shift is much clearer as the Cu content increasing in GP 2.0 composites, 8% Cu content has the best broad elevated background in the visible region due to the presence of Cu state for GP 2.0 composites, indicating the photodeposited different content Cu has clear influence on the optical absorption of TiO_2 nanoparticle and will be favored to enhance the hydrogen evolution under visible light irradiation.

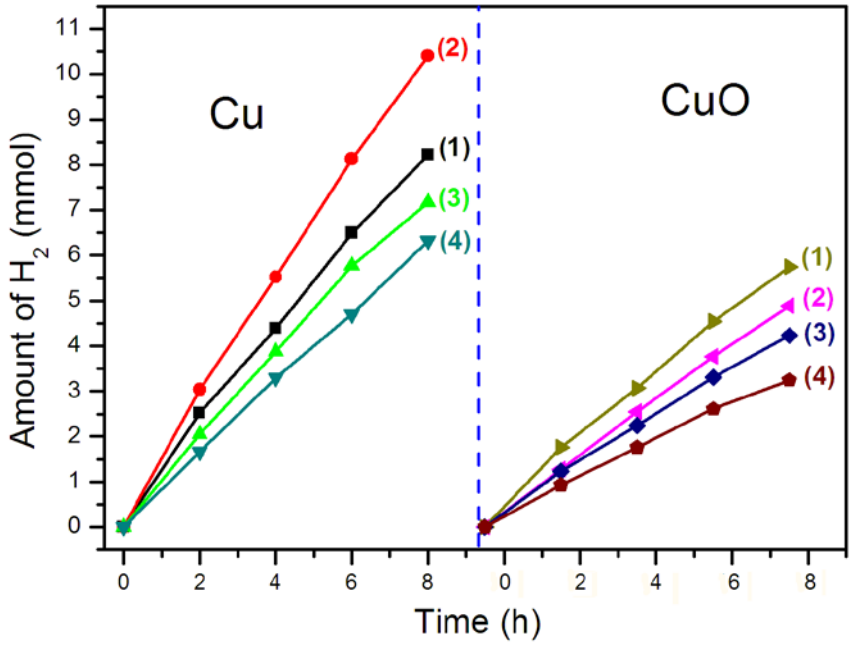

Figure S6. Hydrogen generation capability based on photodeposited Cu loaded GP 2.0 photocatalyst: (1) 1.0% Cu, (2) 1.5% Cu, (3) 2.0% Cu, (4) 3.0% Cu, and CuO loaded GP 2.0 prepared by impregnation method: (1) 1.0% CuO, (2) 1.5% CuO, (3) 2.0% CuO, (4) 3.0% CuO on H_2 generation evolution in methanol aqueous solution under UV−visible light irradiation by 300 W high press Hg lamp.

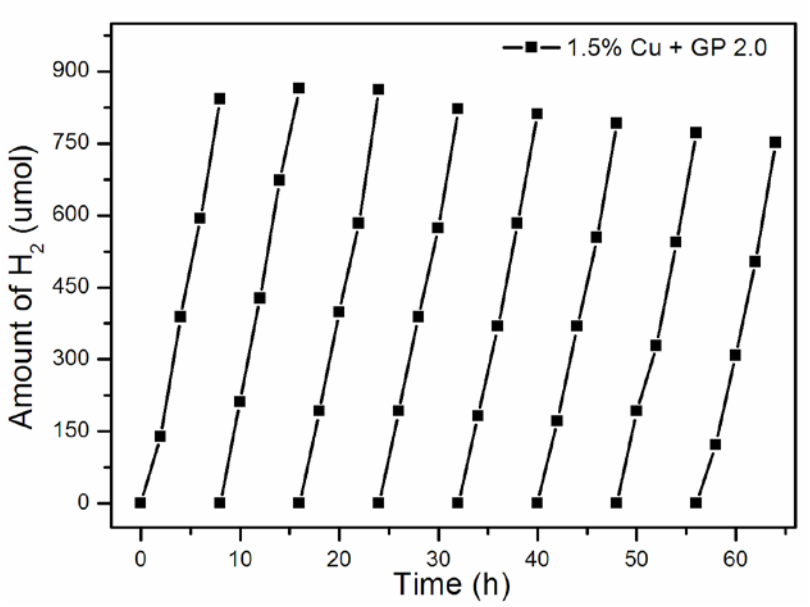

Figure S7. Hydrogen generation capability based on 1.5 % Cu loaded GP 2.0 photocatalysts on H_2 generation evolution in methanol aqueous solution under visible light (λ > 400 nm) by 500 W Xe lamp.

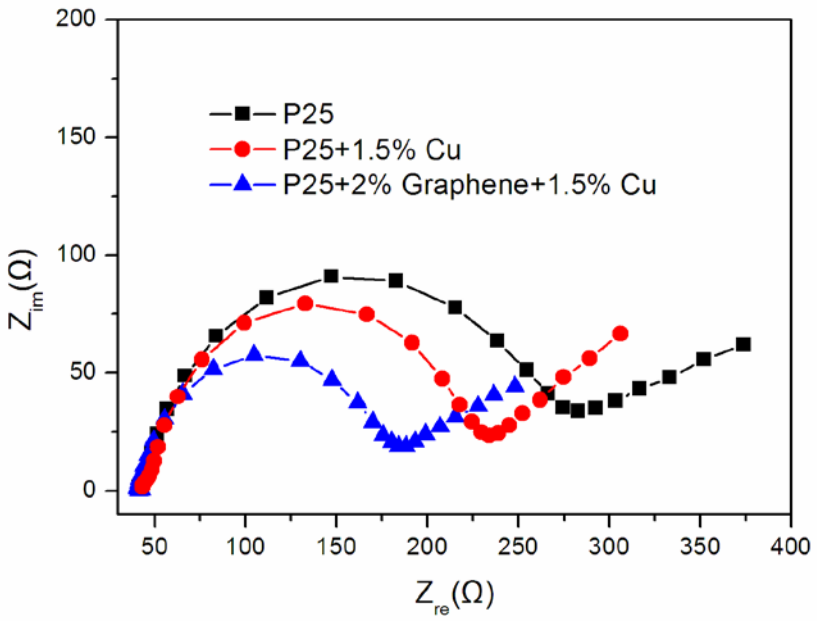

Figure S8. Nyquist plots of electrochemical impedance spectra (EIS) for 1.5% Cu loaded on GP electrodes. The EIS measurements were performed in the presence of 1 mM $K_3[Fe(CN)_6]/K_4[Fe(CN)_6]$ (1:1) mixture as a redox probe in 0.1 M KCl aqueous solution.

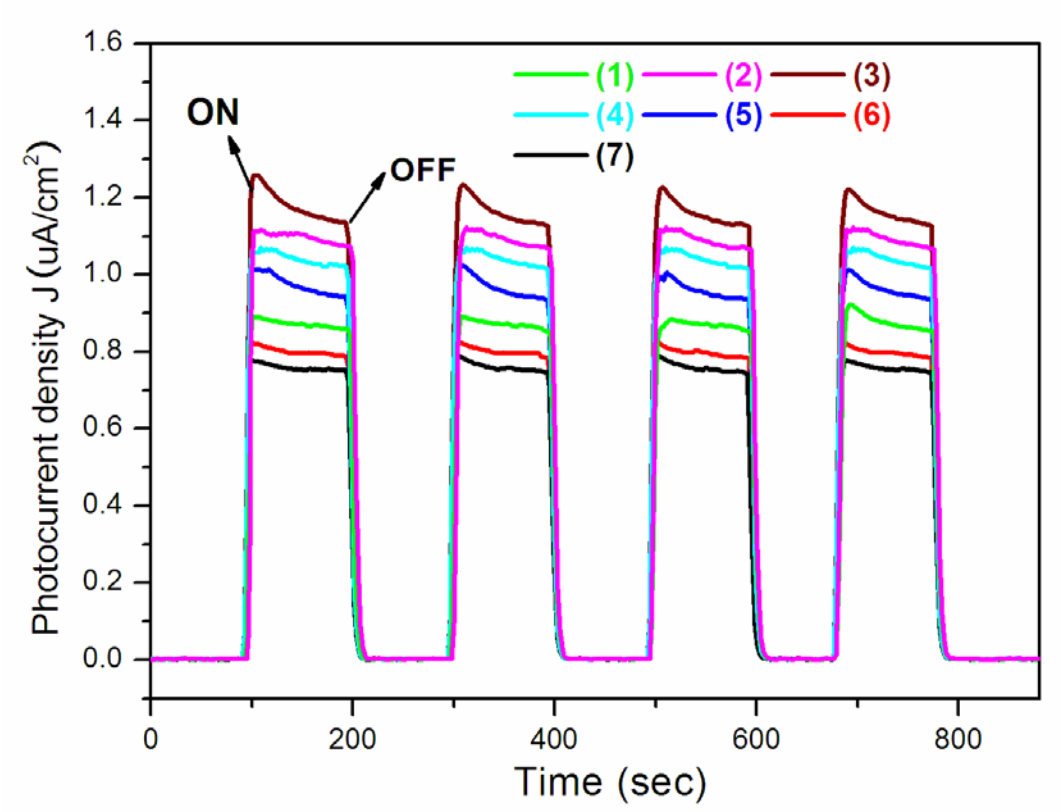

Figure S9. The on−off photocurrent under Xe lamp illumination (1 sun) without bias in a two−electrode configuration for the (1) 0.5% Cu, (2) 1.0% Cu, (3) 1.5% Cu, (4) 2.0% Cu, (5) 3.0% Cu, (6) 5.0% Cu and (7) 8.0% Cu respectively loaded on GP 2.0 composites as photoanodes in 0.1 M KNO_3 solution.

The on−off photocurrent response experiment could demonstrate that different content Cu has deposited on GO 2.0 composites and effectively suppress of photo−excited electron−hole recombination. The results show that photocurrent density enhanced as the Cu content increasing from 0.5% to 1.5%, then decreased obviously when the Cu concentration is higher than 1.5 %, and 8% Cu loaded GP 2.0 exhibited the worst photocurrent density (as shown in Figure S9). The on−off photocurrent results indicate that over−loading of Cu leads to low photocurrent possibly due to the recombination center of photo−induced electron and hole pairs.[5] And the results were in good accordance with the photocatalytic hydrogen evolution capability of photocatalysts.

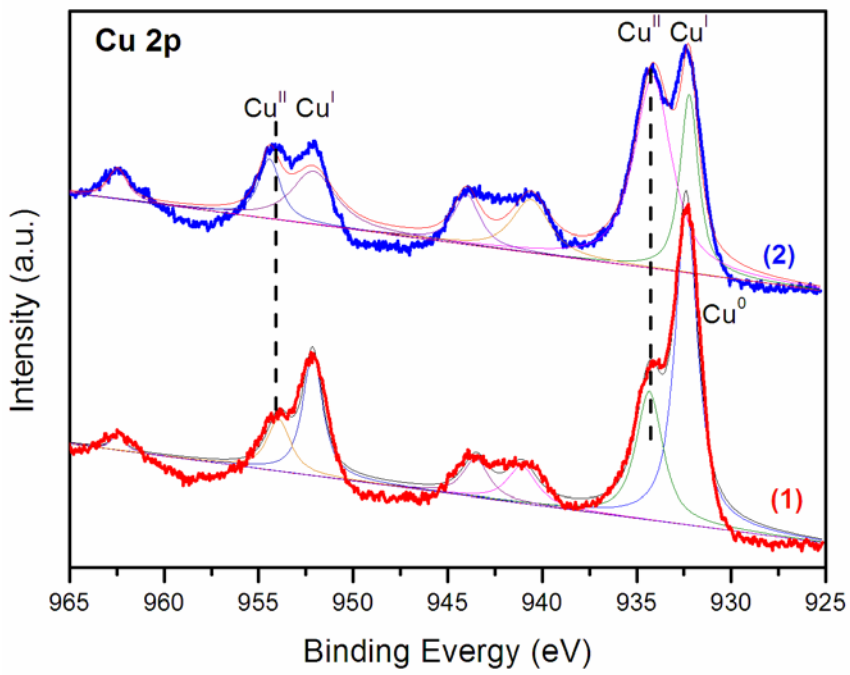

Figure S10. XPS spectra of Cu 2p in the Cu loaded P25–G composites (1) 8% Cu loaded GP 2.0 before irradiation for hydrogen, (2) 8% Cu loaded GP 2.0 after UV–visible irradiation for 64 h.

The Cu $2p_{3/2}$ band at binding energy of 932.2–932.8 eV was assigned to either Cu_2O or Cu (shown in Figure S10). The Cu $2p_{3/2}$ and Cu $2p_{1/2}$ at binding energies of 934 and 953 eV were assigned to CuO. XPS spectra of Cu 2p in the 8% Cu loaded P25–G composites result displayed that after photocatalytic hydrogen evolution after irradiation 64h, the peak of CuO clearly increase,

which illustrated that Cu or Cu_2O could be oxidized during the photocatalytic reaction for hydrogen evolution under UV−visible light irradiation.

References:

[1] W. Fan, Q. Lai, Q. Zhang, Y. Wang, *J. Phys. Chem. C* **2011**, *115*, 10694–10701.

[2] Y. Zhou, Q. Bao, L. A. L. Tang, Y. Zhong, K. P. Loh, *Chem. Mater.* **2009**, *21*, 2950–2956.

[3] O. Akhavan and E. Ghaderi, *J. Phys. Chem. C*, **2009**, *113*, 20214–20220.

[4] Q. Xiang, J. Yu, M. Jaroniec, *Nanoscale*, **2011**, *3*, 3670–3678.

[5] Y. Wu, G. Lu, S. Li, *Catal Lett*, **2009**, *133*, 97–105.